

Physical principles adapted to clinical practice for a theoretical smoke evacuation device in laparoscopic surgery

V. J. Ovejero Gómez^{a,b,*}, V. Ovejero Bermúdez^{a,*} and C. Sainz Fernández^{a,†}

^a*Department of Medical Physics, University of Cantabria,*

^b*Department of General and Digestive Surgery, Marqués de Valdecilla University Hospital,*

Avenida Herrera Oria s/n, 39011, Santander, Spain.

*e-mail: *ovejeroj@unican.es; *victorovejobermudez12@gmail.com; †carlos.sainz@unican.es*

Received 17 July 2024; accepted 31 March 2025

Suboptimal visualization of the surgical field due to smoke generated in any laparoscopic technique, along with the impact on healthcare workers exposed to its toxic particles, has prompted the marketing of various suctioning devices. A limited information on physical basis of these systems has encouraged us to develop a theoretical model that enables a basic experimental recreation of smoke evacuation in pneumoperitoneum.

The cooling effect of the abdominal cavity due to the circulation of insufflated gas and variations in its composition resulting from the operative use of electrocoagulation are the primary factors that lead to the collapse of a circuit designed under laminar flow conditions when an increase in suction flow rate is required to preserve surgical vision. The pressure difference generated in the circuit by tripling its flow induces a change in flow regime, preventing collapse without the need for excessive gas renewal. An analysis of the cross-sectional radius, tube wall composition and absolute roughness of endoluminal surface are conducted to assess performance of our model.

Behavior of fluids in different pathophysiological situations is studied by Science undergraduates, but instructional simulations in the laboratory often fail to transfer this knowledge into the design of practical devices that correlate the statics of an inert material with the variability of a biological system. This theoretical device has been crafted to encourage students interested in the experimental patterns for biomedical applications related to fluid behavior and turnover during minimally invasive procedures involving the peritoneal cavity.

Keywords: Smoke suction; laparoscopy; theoretical device; physical principles; health protective measures.

DOI: <https://doi.org/10.31349/RevMexFis.71.051101>

1. Introduction

A virtual work space based on carbon dioxide (CO₂) insufflation is required in any laparoscopic technique of the abdominal cavity. Surgical procedure safety may be compromised by both body temperature decrease secondary to this insufflated gas and smoke released from tissue electrocoagulation, lengthening the surgical time and demanding a greater turnover of the insufflated CO₂ volume with the potential for the operating room environmental pollution risk by toxic particles.

Conventional electrosurgical devices work based on an electron flow that passes through the patient from an active electrode to a neutral one, generating a variable amount of heat which, according to Joule's law, is influenced by parameters such as current intensity, active electrode size, exposure time, and tissue conductivity [1]. The current intensity generated upon circuit activation by contact of the positive electrode with a specific tissue area determines a local temperature rise with variable effects ranging from protein denaturation coagulation to tissue carbonization for a temperature range oscillating between 40 and 150°C. This thermal variation will result in the release of energy, water vapor, and a suspension of chemical and biological particles that will mix with insufflated CO₂, requiring its evacuation to preserve the visibility of the operative field. Surgical team exposure to this new fluid generates an epithelial inflammatory response with potential local and systemic clinical manifestations, once the

alveolar-capillary membrane is surpassed, as well as a potential carcinogenic, neurotoxic and infectious effect [2,3].

Surgical smoke has been found to contain over 150 chemical components, whose concentration varies depending on the type of destroyed tissue, and viable infectious and tumoral biological material; which together do not exceed 5% of its composition [4]. Despite this small proportion, it is considered that the smoke released from one gram of tissue is equivalent to the mutagenic effect of inhaling three to six unfiltered cigarettes, and an eight-hour exposure is equivalent to smoking 27-30 cigarettes [5,6]. These similarities are dramatic in laparoscopic procedures because constant opening of the working trocars results in direct exposure to smoke expelled due to increased intra-abdominal pressure, considering the limited protection offered by standard surgical masks against aerosol inhalation [7].

Currently, there is a significant limitation in characterizing the full spectrum of particles in surgical smoke despite the accuracy of some instruments to discriminate mass, volume and number concentrations of particles with an aerodynamic diameter (ϕ_{aer}) below one micrometer. The various filters and extractors used for surgical smoke have the capacity to remove 90% of particles but are ineffective for those with $\phi_{\text{aer}} > 12 \mu\text{m}$ [7,8]. On the other hand, there is a lack of a universal specific regulation regarding the evacuation of this smoke, with only recommendations aimed at improving environmental quality within the facility through devices that

maintain a unidirectional laminar flow [9, 10]. In this context, various international healthcare organizations adhere to recommending the systematic use of individual protective measures.

Few research studies on suction devices in the operating field are available, and none have evaluated the minimum suction flow necessary for effective smoke evacuation [11]. This fact has led to the technical documentation of many devices being empirical, based on simulations. This deficiency and the legal gap regarding its mandatory implementation have generated some reluctance to invest economically in many hospital centers, thus favoring the development of artisanal models.

We propose the theoretical modeling of a rudimentary device to understand the physical principles underlying its operability and the relevant modifications contributing to its optimization. This suggestion could foster the initiation of controlled clinical trials assessing the efficiency and enhancement of various existing devices on the market, as well as their integration into basic laparoscopic instrumentation as a protective measure for the involved healthcare personnel.

2. Modeling of the experimental setup

2.1. Translation from clinical environment to surgical simulation

An experimental surgical smoke suction device has been designed based on the ergonomic guidelines of laparoscopic surgery and pneumoperitoneum conditions in clinical practice. The surgical table height has been set at 0.76 m to accommodate the average height of the surgical team, which is 1.68 m. This aspect takes into account that the ergonomic position for holding instruments requires a 120° elbow flexion so that the height of the hand represents 80% of the length between the elbow and the floor [12, 13].

Abdominal cavity distention typically geometrically resembles an ellipsoid, but considering the significant individual variability among patients, the model has been simplified by assuming that all three diameters could have the same length. The experimental volume has been set at 3.5 L based on the mean volume of insufflated CO_2 for a predetermined intra-abdominal pressure of 12 mmHg in a record of 40 consecutive patients undergoing laparoscopic cholecystectomy as the reference procedure. The calculation of the post-insufflation mean anteroposterior diameter of the abdomen has been estimated at 0.19 ± 0.03 m when the gas was at rest in a group of patients who had presented a volume of ± 0.1 L relative to the indicated value. This diameter has been standardized across all three spatial axes. Our smoke evacuation device was arbitrarily placed 0.05 m below the level of maximum abdominal distention (Fig. 1).

A suction flow rate (Q) of $8.75 \cdot 10^{-5} \text{ m}^3/\text{s}$ (5.25 L/min) has been established according to our clinical experience, assuming that evacuating 25% of the insufflated volume within

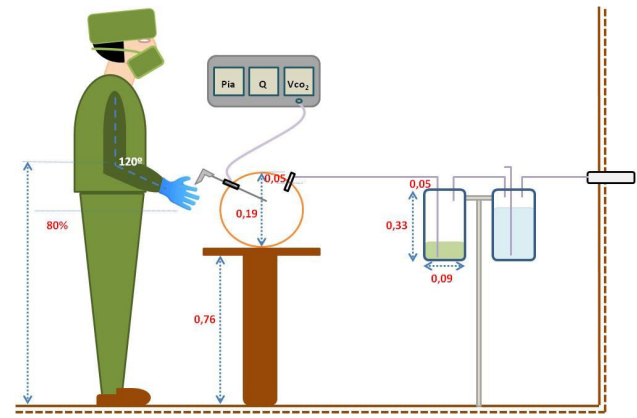


FIGURE 1. Schematic drawing of the ergonomic relationships between the surgeon and the surgical table regarding the spherical simulation of the insufflated abdominal cavity connected to the suction circuit (dimensions have been expressed in meters). The left canister works as a filter. The aspiration transmitted to the patient has been determined by the height of the rod in the right canister.

10 seconds is sufficient to remove the necessary smoke to maintain optimal visibility and facilitate a gradual recovery of the pneumoperitoneum without abrupt variations in body temperature. This consideration also takes into account that the cycling rate of most laparoscopic equipment is 3:1.

Furthermore, an ideal intra-abdominal pressure (P_1) of 1599.87 Pa (12 mmHg) was agreed upon to avoid systemic effects of abdominal hypertension on the patient, although values between 1066.58 and 1866.51 Pa (8 and 14 mmHg) are accepted in clinical practice.

Our experimental device was designed from materials commonly available in the surgical area of any hospital center. The internal diameter of the circuit was 0.006 m to allow its connection to trocars marketed with 0.01 m section, supplied with a valve preventing gas leakage during simultaneous use with standard laparoscopic instrumentation with 0.004 m section.

The smoke evacuation system was comprised by a module connecting the abdominal cavity to a particulate seal, which was placed in a 0.33 m height and 0.043 m radius cylindrical canister. This seal was composed of a 0.5 L solution consisting of 25 mL sodium hypochlorite and 475 mL saline solution, resulting in a column with 0.09 m height and 770.86 Pa hydrostatic pressure (P_s). This pressure was calculated using the formula $P_s = \rho gh$, where ρ (1006 kg/m^3) is the density of the sodium hypochlorite and saline solution mixture, g is referred to gravitational acceleration, and h means the height of the solution for a cylindrical volume.

Its total length was established as 1.2 m to ensure a properly width from a hypothetical patient to the seal in accordance with abdominal distention and the ergonomic height of the surgical table (Fig. 1). The circuit wall was assumed to be composed of polyethylene with a $4.3 \cdot 10^{-6} \text{ m}$ inner surface standardized roughness (ε) based on the average value reported in commercially available tables for this material [14].

This module has been assembled to a second canister with the same dimensions to predetermine a suction pressure for the circuit, thus avoiding the need for the Venturi effect provided by a flowmeter, not always available. The suction pressure of the system (P_2) was defined by the pressure difference between the central suction in the operating room, regulated through the saline solution column in the second canister (P_{asp}), and the P_s provided by the particulate seal. In this second canister, a rod was placed as an atmospheric ventilation system to ensure that the value of the suction pressure was determined by the height of the saline column counteracting an average suction pressure of 60000 Pa coming from the operating room central circuit. Both this column and the particulate seal bubbling were indicative of the right functioning of the system.

Under the specified flow rate and circuit diameter conditions, if the aspirated gas is considered to be an incompressible Newtonian fluid assuming approximately constant density and viscosity throughout the flow, the P_{asp} (2317.16 Pa) could be determined using Poiseuille's law, since the flow would exhibit a Reynolds number (Re) of 1809 for an average velocity (\bar{v}) of 3.09 m/s according to the expression

$$\bar{v} = \frac{Q}{\pi r^2}, \quad (1)$$

where Q is the flow rate and r is the cross-sectional radius of the circuit.

Poiseuille equation ($\Delta P = R \cdot Q$), with R being the resistance offered by the aspiration circuit, is equivalent to

$$\Delta P = \frac{8\eta l}{\pi r^4} Q, \quad (2)$$

where η is the viscosity of the fluid, l is the length of the circuit and $\Delta P = P_1 - P_2$; with $P_1 = P_{ia}$ and $P_2 = P_{asp} - P_s$, so that it can be expressed as

$$[P_1 - (P_{asp} - P_s)]\pi r^4 = 8\eta l Q. \quad (3)$$

The P_{asp} allowed the estimation of the height of the saline solution column ($\rho = 1005 \text{ kg/m}^3$) as 0.24 m due to the effect of Stevin's hydrostatic pressure principle on the column.

2.2. Surgical smoke characterisation

Pneumoperitoneum is usually performed with CO_2 in surgical procedures since its high diffusion coefficient compared to other blood gases promotes rapid absorption into the circulatory system and easy monitoring as it is eliminated via the respiratory route. Insufflation into the abdominal cavity is typically conducted at 20-25°C, leading to a decrease in body temperature exacerbated by the convective effect of flow and fluid evaporation through the peritoneum due to the turbulence of the gas pumped under pressure. Furthermore,

TABLE I. Molecular mass of the main chemical components of surgical smoke.

Chemical Component	$M / \text{g} \cdot \text{mol}^{-1}$	Chemical Component	$M / \text{g} \cdot \text{mol}^{-1}$
Acrolein ($\text{C}_3\text{H}_4\text{O}$)	56.06	Styrene (C_8H_8)	104.11
Acetonitrile ($\text{C}_2\text{H}_3\text{N}$)	41.05	Formaldehyde (CH_2O)	30.03
Acetylene (C_2H_2)	26.04	Indole ($\text{C}_8\text{H}_7\text{N}$)	117.15
Acrylonitrile ($\text{C}_3\text{H}_3\text{N}$)	53.06	Isobutane (C_4H_{10})**	58.12
Benzaldehyde ($\text{C}_7\text{H}_6\text{O}$)	106.12	Furfural ($\text{C}_5\text{H}_4\text{O}_2$)	96.08
Palmitic acid ($\text{C}_{16}\text{H}_{32}\text{O}_2$)	256.43	Methanol (CH_4O)	32.04
Benzene (C_6H_6)	78.11	2-methylpropane (C_4H_{10})***	58.12
Benzonitrile ($\text{C}_7\text{H}_5\text{N}$)	103.04	Methane (CH_4)	16.04
Butadiene (C_4H_6)	54.09	3-methylbutane (C_5H_{12})	86.2
N-butane (C_4H_{10})	58.12	2-methylfuran ($\text{C}_5\text{H}_6\text{O}$)	82.1
3-butenitrile ($\text{C}_4\text{H}_5\text{N}$)	69.11	Phenol ($\text{C}_6\text{H}_6\text{O}$)	94.11
Carbon disulfide (CS_2)	76.14	Alkylbenzene sulfonate ($\text{C}_{12}\text{H}_{25}\text{-C}_6\text{H}_4\text{-SO}_3\text{H}$)	342.4
Carbon monoxide (CO)	28.01	Propene (C_3H_6)	42.08
o-cresol, p-cresol, m-cresol ($\text{C}_7\text{H}_8\text{O}$)	108.14	2-propene nitrile ($\text{C}_3\text{H}_5\text{N}$)	53.06
Hydrogen cyanide (HCN)	27.03	Pyridine ($\text{C}_5\text{H}_5\text{N}$)	79.1
1-decene ($\text{C}_{10}\text{H}_{20}$)	140.27	Pyrrole ($\text{C}_4\text{H}_5\text{N}$)	67.09
Ethane (C_2H_6)	30.07	Toluene (C_7H_8)	92.14
Ethylene (C_2H_4)	28.05	Xylene (C_8H_{10})	106.16
Ethylbenzene (C_8H_{10})*	106.17	Water vapor (H_2O)	18.02

*Ethylbenzene is part of the xylene mixture, which contains 3 isomers and 6 to 15% ethylbenzene.

**Isobutane (i-butane) is an isomer of normal butane (n-butane). It is converted to n-butane by isomerization.

***2-methylpropane and butane are nonpolar and have the same molecular formula. However, butane has a higher boiling point (-0.5°C vs -11.7°C).

the CO₂ has got a very low water concentration, which induces desiccation and desquamation of mesothelial cells that become part of the intra-abdominal gas. This temperature difference also contributes to the defective display of the surgical field due to fogging of the optical lens [15].

The smoke generated by the effect of monopolar electrocoagulation on tissues consisted of water vapor (95%), particles and biological agents (5%). An average concentration of 100000 particles/(cm³ · h) has been taken as a general reference, equivalent to the minimum average generated in surgical electrocauterization. Most of the particles have sizes ranging from 0.025 to 0.1 μm [16, 17]. Table I shows a sample of the most representative smoke molecules that have been used to quantify the physical characteristics of the treated fluid [18, 19].

The aspirated gas has been considered a fluid composed of CO₂ and smoke. Its density ($\rho = 1.29 \text{ kg/m}^3$) was obtained from the mixed density of equal volumes of CO₂ on one side and water vapor/particles on the other. The viscosity ($\eta = 1.32 \cdot 10^{-5} \text{ Pa}\cdot\text{s}$) was calculated from the mixture of the same components using the Arrhenius equation, as it is a non-heavy fluid, according to the expression

$$\ln \eta = \sum_{i=1}^N X_i \ln \eta_i,$$

where X_i is the mole fraction $X_i = n_i / \sum_{j=1}^N n_j$ and the summations account for the elements considered in the aspirated gas.

The viscosity value may undergo slight variations in vivo due to the temperature difference between the abdominal cavity, estimated to be around 20°C as a result of the cooling effect during CO₂ insufflation, and the fluid pathway through the circuit. However, a constant temperature throughout the circuit has been assumed to facilitate theoretical modeling.

3. Analytical modeling of the circuit

3.1. Approximation of the model to laminar or turbulent flow

The linear arrangement of the circuit between the patient and the canisters, along with the predetermined conditions in the device design and the physical characteristics of the treated fluid, has allowed for a first approximation to be made from the perspective of a laminar flow regime, ensuring optimal visibility and recovery of the initial P_{1a} without interrupting the surgical procedure. The circuit suction pressure (P_2) and the circuit pressure difference with respect to the intra-abdominal pressure (ΔP) have been calculated using Eqs. (2) and (3). This analysis has been compared with an evaluation of the model when fluid evacuation is subjected to the passive effect of gravity.

In a second stage, the system was considered under turbulent flow conditions to obtain a more realistic representation of clinical practice. The calculation of ΔP , that delin-

eates the transition from laminar to turbulent flow, was derived from Eq. (2) and the equation corresponding to Re , as follows

$$Q = \frac{\pi r \eta Re}{2\rho} \Rightarrow \Delta P = \frac{4\eta^2 l Re}{\rho r^3}, \quad (4)$$

On the other hand, it must be considered that the flow rate depends on fluid resistance for a constant pressure gradient, as described by Poiseuille's equation. This relationship implies that improving the efficiency of the original circuit while maintaining its length and internal diameter, an increase in its flow rate inherently requires an increase in suction pressure to accommodate the range of intra-abdominal pressures allowed under safe conditions. Therefore, the variability of intraoperative circumstances in any laparoscopic procedure necessarily requires considering a circuit operating under turbulent flow conditions to meet any demand for evacuation flow.

In this scenario, it has been arbitrarily established that an increase in flow rate up to $2.5 \cdot 10^{-4} \text{ m}^3/\text{s}$ (15 L/min) for the same system section diameter could be sufficient to effectively evacuate surgical smoke, based on experiments provided by other authors [20]. This increase in flow rate implies a change in \bar{v} to 8.84 m/s according to Eq. (1), which results in the presence of a turbulent flow regime in the circuit ($Re = 5167.38$). The fluid analysis under a turbulent regime was performed using the Fanning equation [21, 22]:

$$\Delta P = \frac{f v^2 l}{r}, \quad (5)$$

where f is the Fanning friction factor.

Newton's second law, when taking viscosity into account, does not hold in a turbulent regime, making the analytical calculation of velocity difficult, especially for high values due to the chaotic movement of fluid molecules. However, it can generally be assumed that all point velocities are equal to each other and to the average velocity. This assumption allows the definition of linear velocity (v) in the same terms as in Eq. (1), according to which

$$Q^2 = \frac{\Delta P \pi^2 r^5}{f l}, \quad (6)$$

where r and l must be expressed in metres. In this way, the internal radius of the circuit is the primary determinant of the system's resistance, as it influences the flow rate to the fifth power of its value.

In our case, the calculation of the Fanning factor [23], considering a rough internal surface of a polyethylene circuit, was performed using Eq. (7), valid for a Re between $5 \cdot 10^3$ and 10^8 :

$$f = \frac{0.25}{\left[\log \left(\frac{\epsilon}{3.7} + \frac{5.74}{Re^{0.9}} \right) \right]^2}, \quad (7)$$

where D is the diameter of the circuit. The obtained value of f was verified using the logarithmic coordinates of the Moody diagram.

Additionally, this mathematical formulation has been used to analyze possible differences in ΔP based on variations in the endoluminal ε , depending on whether the circuit is composed of polyethylene or flexible rubber. The extreme values of ε are $1.5 \cdot 10^{-6}$ - $7 \cdot 10^{-6}$ and $6 \cdot 10^{-6}$ - $7 \cdot 10^{-5}$ m, respectively [14].

3.2. Impact of circuit diameter on both flow regimes

A clear influence of the internal diameter on both Q and the ΔP developed by the circuit is observed, based on their relationship with Poiseuille's law or the Fanning equation. Differences in these parameters have been evaluated depending on whether the flow is laminar or turbulent.

In the case of laminar flow, changes in Q resulting from a hypothetical decrease in the internal diameter of the circuit under the specified conditions can be deduced from the following expression

$$\frac{Q'}{Q} = \frac{r'^4}{r^4},$$

resulting in Q' and r' as the new flow rate and internal radius of the circuit, respectively; where r' is defined as $r' = r - x \cdot r$, with x referring to the percentage variations in the radius of the circuit. This equality would imply that

$$\frac{Q'}{Q} = \frac{[r(1-x)]^4}{r^4} = (1-x)^4; \quad Q' = Q(1-x)^4. \quad (8)$$

Similarly, modifications in the internal diameter of the circuit will affect ΔP for a constant flow rate preset at 5.25 L/min. Its value can be calculated using the following equivalence ratio

$$\frac{\Delta P'}{\Delta P} = \frac{r^4}{r'^4},$$

where $\Delta P'$ is the pressure gradient for the changes in the internal radius of the circuit, with r' taking the same form as previously expressed.

$$\frac{\Delta P'}{\Delta P} = \frac{r^4}{[r(1-x)]^4} = \frac{1}{(1-x)^4} = (1-x)^{-4},$$

$$\Delta P' = \Delta P(1-x)^{-4}. \quad (9)$$

The equivalence ratio for Q and ΔP in a circuit under turbulent flow conditions subjected to variations in its internal diameter can be established in a similar manner, considering that the influence of the radius is given by its fifth power according to the Fanning equation. Thus, the reduction in the internal radius of the circuit could be correlated with these variables using the same expression for r' employed in the laminar regime, such that:

$$\frac{Q'^2}{Q^2} = (1-x)^5 \Rightarrow Q' = Q(1-x)^{5/2}, \quad (10)$$

and

$$\frac{\Delta P'}{\Delta P} = (1-x)^{-5} \Rightarrow \Delta P' = \Delta P(1-x)^{-5}. \quad (11)$$

4. Results and discussion

4.1. Evolutionary adequacy of the model to real-world circumstances

The analysis of the proposed suction model, based on the principles of laminar flow and using Eqs. (2) and (3), determined a value of $P_2 = 1556.3$ Pa from a $P_{asp} = 2327.16$ Pa and a $P_s = 770.86$ Pa, from which $\Delta P = 43.57$ Pa is deduced, considering the circuit as linear between the abdomen outlet and the central suction, as shown in Fig. 1.

In contrast, placing the particulate seal at ground level as a passive drainage system would create a height difference relative to the ergonomic position of the patient on the surgical table, resulting in a $\Delta P = 819.57$ Pa due to gravity in accordance with the fundamental law of hydrostatics, leading to higher suction flow rates. Its proper functioning is also contingent upon maintaining a linear system between the abdomen outlet and the particulate seal, as any stenosis due to kinking would increase resistance and, consequently, alter the pressure gradient.

The internal diameter of the circuit is one of the main determinants of flow, as for the same ΔP , a larger diameter results in lower circuit resistance and a higher flow rate [21,24]. In the suction circuit, this relationship becomes particularly significant for sections larger than 6 mm [Fig. 2a)]. Conversely, the circuit subjected solely to gravity experiences much more significant increases in flow for the same diameter [Fig. 2b)] due to the influence of the height difference between the abdomen, positioned on the surgical table, and the particulate seal with respect to ΔP . The relationship between the velocity and flow rate in a circuit with a constant diameter determines that at higher fluid velocities, even without changes in its physical characteristics, the Re increases until values indicative of a turbulent regime are reached.

In this context, changes in the physical characteristics of the fluid due to prolonged use of electrocoagulation are usually attributed to the large volume of smoke generated, which increases the proportion of water vapor due to humidity with relative to the number of particles contained. This variation in the fluid is associated with an increase in density and, to a lesser extent, viscosity, which could potentially lead to clogging of the suction system under laminar flow conditions. A higher suction flow rate than initially planned could address this issue but would also result in the transition to a turbulent flow regime.

Additionally, certain inherent factors of the surgical procedure also induce a turbulent regime by increasing fluid velocity. The loss of muscle relaxation in the abdominal wall causes an increase in ΔP due to elevated intra-abdominal pressure, leading to a higher flow rate without modifications in the system's resistance.

Both considerations suggest that our suction device operates within a delicate balance regarding suction efficiency under laminar flow conditions. Its intrinsic characteristics and

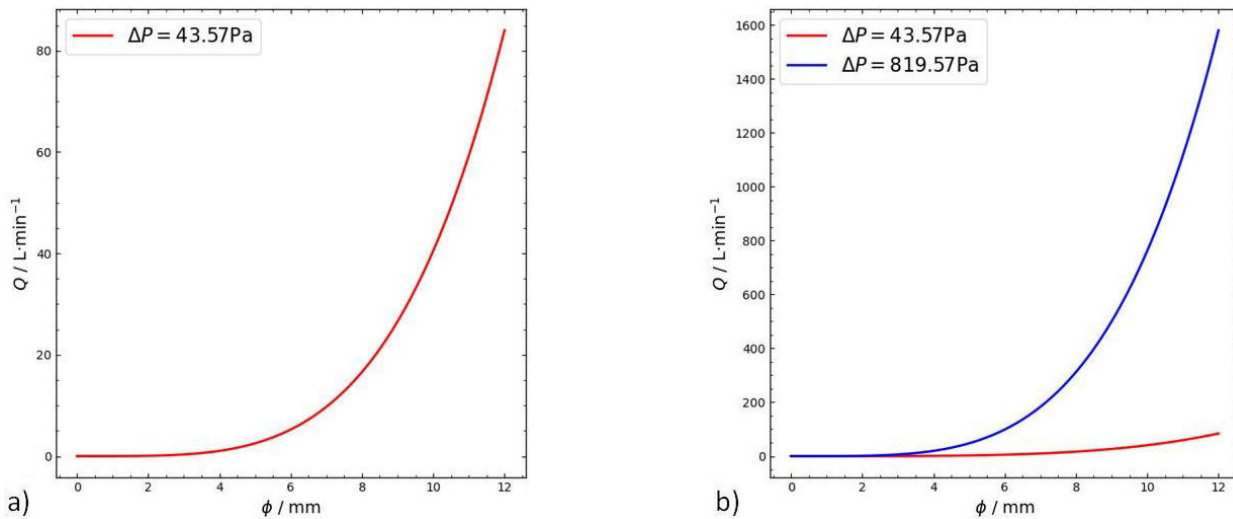


FIGURE 2. Influence of the internal diameter on the suction flow rate for a circuit subjected to active aspiration, shown in red a), and its behavior with respect to passive drainage by gravity, shown in blue b). In both figures, the theoretical curve of Eq. (2) has been represented in relation to flow rate and diameter for two different ΔP values.

the properties of the treated fluid allow for a maximum ΔP of 55.4 Pa when analyzed in relation to Poiseuille's law and the concept of Re , as expressed in Eq. (4). Any further increase in pressure difference would indicate a transition to a turbulent regime.

Finally, the relationship between intra-abdominal pressure and suction flow rate, according to Poiseuille's law for the designed circuit, indicates that P_{ia} values lower than the predetermined threshold (12 mmHg) are associated with a reversal of Q , which would also render the system inoperative. Conversely, a linear increase in flow rate occurs with increases in P_{ia} , as described by Eq. (3), provided that no variations in the internal diameter take place.

The aforementioned conditions, the need for an effective immediate response and the surgeon's desire for autonomy in handling the instruments make the described smoke evacuation system impractical. A model that allows for better adjustment of the suction flow rate, based on the requirements of the surgical procedure, would be necessary to prevent excessive replacement of CO_2 volume or circuit collapse. Optimizing the system under the guidelines of a turbulent regime, referencing the proposed Q of $2.5 \cdot 10^{-4} \text{ m}^3/\text{s}$ and \bar{v} of 8.84 m/s, could provide a reasonable solution, but

it has the drawback of resulting in more pronounced changes in flow rate for the same internal diameter of the circuit, as indicated by the development of Eq. (5).

In these circumstances, the fluid flow through the circuit also results in a hydraulic head loss due to friction against its walls. This pressure drop along a constant length of circuit is directly related to the resistance exerted by the roughness of its internal surface, shown by f , and the average fluid velocity; varying inversely with its internal diameter, as described by expression (5).

The f for the section diameter and ε of the circuit reached a value of 0.038 according to Eq. (7), and the value of ΔP increased to 1187.81 Pa according to Eq. (5), which highlights that the new circuit model improves its operability and achieves greater sensitivity to variations in the internal radius, resulting in a much steeper increase in flow rate for smaller internal diameters than those observed in the laminar regime (Fig. 3).

The variations in the absolute roughness of the pipe material for a constant internal diameter showed discrete pressure differences in the circuit, more pronounced with higher absolute roughness when the material was elastic rubber, as shown in Table II.

TABLE II. Pressure variations (ΔP) in the circuit according to different absolute endoluminal roughnesses for two possible pipe materials.

Material	ε (m)	f	ΔP (Pa)	Q (L·min ⁻¹)
Polyethylene	$1.5 \cdot 10^{-6}$	0.038	1156.55	15
	$4.3 \cdot 10^{-6}$	0.038	1187.81	15
	$7 \cdot 10^{-6}$	0.039	1219.07	15
Flexible rubber	$6 \cdot 10^{-6}$	0.039	1219.07	15
	$3.8 \cdot 10^{-5}$	0.045	1406.7	15
	$7 \cdot 10^{-5}$	0.05	1562.91	15

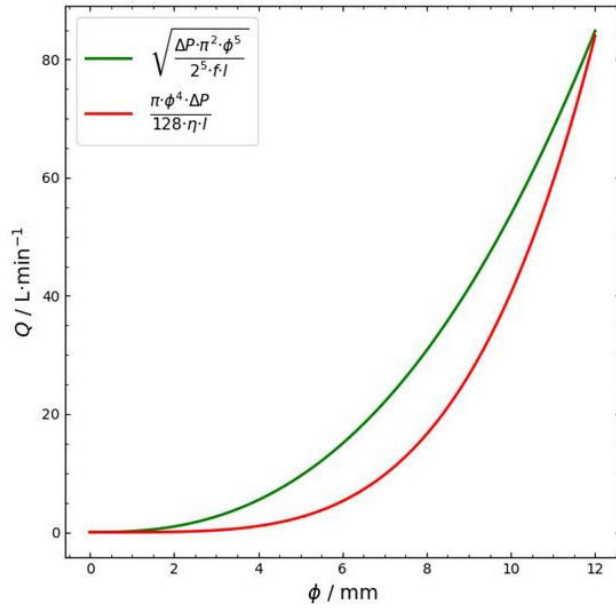


FIGURE 3. Relationship between the internal diameter (ϕ) and the suction flow rate (Q) for laminar (red) and turbulent (green) flow in a suction circuit. The theoretical curve based on Eqs. (2) and (6) has been represented with a ΔP of 43.57 Pa for the laminar regime and 1187.81 Pa for the turbulent regime.

4.2. Internal diameter effect on circuit flow and pressure

A laminar flow, according to Eq. (9), for the designed circuit with $r = 0.003$ m and $Q = 5.25$ L/min means that a progressive reduction in the circuit's diameter leads to dramatic decreases in flow rate due to the fourth power effect of its internal radius. For instance, a 20% reduction decreases the flow by 59.05% from its original value, while reductions in diameter exceeding 50% limit the flow to values below 10% of the initial flow rate. This phenomenon is only achievable when the internal diameter of the circuit is uniformly reduced along its entire length; as in cases of localized stenosis or bends, the principle of continuity would still be preserved.

Similarly, these circuit conditions for a $\Delta P = 43.57$ Pa mean that a 20% reduction in diameter results in a ΔP of 106.37 Pa, while a 50% reduction generates 697.12 Pa. This indicates that the system requires a 16-fold increase in ΔP to maintain a constant flow rate and viscosity when the circuit radius is reduced to half of its initial value.

The analysis of the circuit under conditions of $Q = 15$ L/min and $\Delta P = 1187.81$ Pa for a turbulent regime, according to Eq. (10), indicates a lower flow rate loss compared to the laminar regime for the same reduction in internal diameter (42.74% vs 59.05% and 82.33% vs 93.75% for a 20% and 50% decrease in circuit diameter, respectively). The influence of the internal radius variations in Eq. (11) also demonstrates an increase in ΔP for the turbulent regime, but in this case, its value increases up to 32 times compared to the initially proposed value in this model ($\Delta P = 1187.81$ Pa).

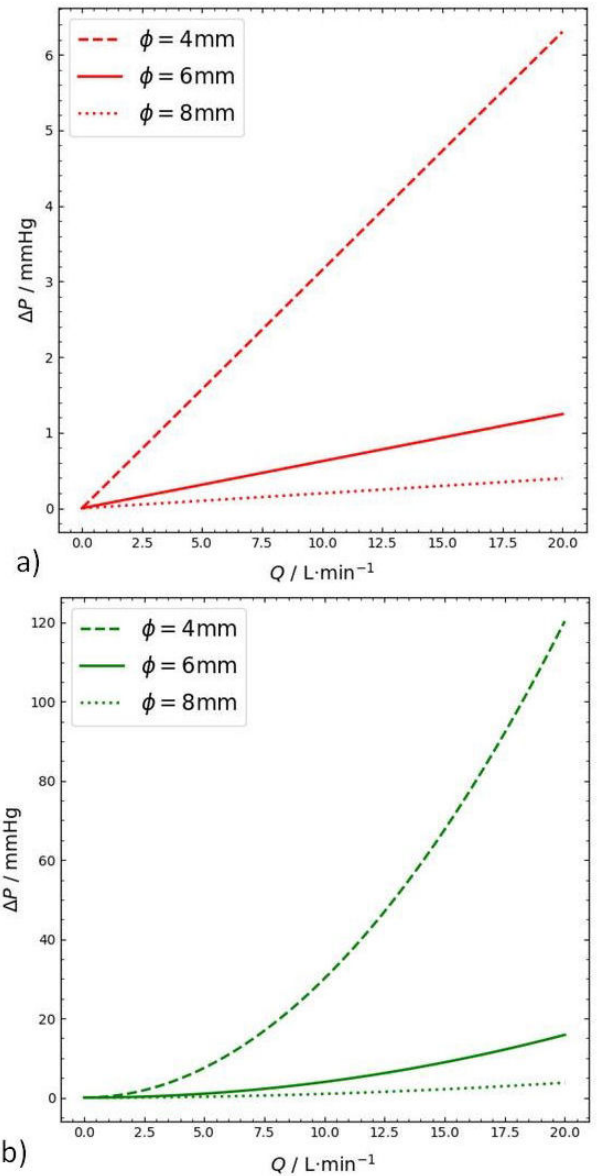


FIGURE 4. Relationship between the suction flow rate (Q) and the pressure difference (ΔP) between the abdominal cavity and the system, according to the theoretical curve of Eqs. (2) and (6), for a circuit with different internal diameters, whether in a laminar (4a) or turbulent regime (4b).

The relationship between Q and ΔP with respect to the reduction of the internal radius of the circuit in the assumed laminar and turbulent regimes can be observed in Table III.

The reduction in the internal diameter of the circuit is associated with an increase in resistance, which becomes more evident in the turbulent regime for the same suction flow rate, as shown in Fig. 4. Conversely, an increase in the circuit diameter tends to result in a more aerodynamic flow.

Therefore, the internal diameter of circuit plays a crucial role in fluid behavior. A smaller diameter results in greater system resistance as the suction flow rate increases, promoting the intensification of turbulent flow. This resistance is proportional to the fifth power of the lumen radius according to Fanning's equation.

TABLE III. Effect of decreasing the internal radius of the suction circuit under a laminar regime ($Q = 5.25$ L/min and $\Delta P = 43.57$ Pa) or turbulent regime ($Q = 15$ L/min and $\Delta P = 1187.81$ Pa), respectively.

REGIME:	Laminar		Turbulent	
Radius reduction (%)	Q (L·min ⁻¹)	ΔP (Pa)	Q (L·min ⁻¹)	ΔP (Pa)
10	3.44	$6.6 \cdot 10$	11.53	$2 \cdot 10^3$
20	2.15	$1.1 \cdot 10^2$	8.59	$3.6 \cdot 10^3$
25	1.66	$1.4 \cdot 10^2$	7.31	$5 \cdot 10^3$
50	0.33	$7 \cdot 10^2$	2.65	$3.8 \cdot 10^4$
75	0.02	$1.1 \cdot 10^4$	0.47	$1.2 \cdot 10^6$

Similarly, conditions that increase the viscosity of fluid, such as a higher concentration of particles in smoke due to excessive electrocoagulation or increased density due to circulating at lower temperatures, may also contribute to the promotion of turbulent flow.

5. Conclusions

A theoretical smoke suction device has been developed based on models used in laparoscopic abdominal procedures. An approximation to real-world conditions, along with the influence of the intrinsic characteristics of the designed circuit, indicates the superiority of turbulent flow in maintaining operability.

We have used readily available materials to facilitate experimentation. A specification of the prototype and the surgical scene was provided to encourage physics students to apply it in various scenarios, allowing for a comparative analysis between theoretical data and laboratory measurements. The results presented aim to highlight the versatility of biological systems in contrast to static models described in textbooks, emphasizing the importance of experimentation in overcoming the limitations of theoretical models.

In clinical practice, individual variability in the abdominal cavity and biomechanical changes during the progression of surgical and anesthetic techniques lead to fluctuations in intra-abdominal pressure and variations in the composition of the aspirated fluid throughout the procedure. Further analysis of prototypes capable of regulating the suction flow rate based on procedural demands would be of interest, as well as an evaluation of the influence of length, section diameter,

and endoluminal surface roughness on efficiency and safety, without requiring excessive turnover of insufflated fluid.

The physical conditions of insufflated CO₂ make it difficult a proper vision of the operative field and promote hypothermia, postoperative adynamic ileus, desquamation of mesothelial cells and adhesions due to loss of peritoneal integrity. The recent incorporation of gas heating and humidification devices in new laparoscopic equipment appears to be achieving a positive effect in preventing these complications [15, 25]. The incorporation of these new enhancement elements into experimental simulations could optimize the conditions described and establish guidelines for a universal clinical model in accordance with current surgical needs and recommended preventive measures.

Acknowledgments

The authors would like to express their gratitude to all the surgical staff at the Marqués de Valdecilla University Hospital in Santander, who have generously supported this project by allowing the use of their anthropometric conditions and their own records on abdominal distensibility in laparoscopic surgery to contextualize this theoretical device in routine clinical practice.

Author declarations

Conflict of interest

The authors declare no conflicts of interest in the present article.

1. I. Alkatout, T. Schollmeyer, N.A. Hawaldar, N. Sharma, and L. Mettler, Principles and safety measures of electrosurgery in laparoscopy, *JSLs* **16** (2012) 130, <https://doi.org/10.4293/108680812X13291597716348>.
2. M. Dobrogowski, W. Wesolowski, M. Kucharska, A. Sapota, and L.S. Pomorski, Chemical composition of surgical smoke formed in the abdominal cavity during laparoscopic cholecystectomy - Assessment of the risk to the patient, *Int J Occup*

Med Environ Health **27** (2014) 314, <https://doi.org/10.2478/s13382-014-0250-3>.

3. S.M. In *et al.*, Experimental study of the potential hazards of surgical smoke from powered instruments, *Br J Surg* **102** (2015) 1581, <https://doi.org/10.1002/bjs.9910>.
4. A. Mollov, A. Echevarria, S. Herrera, C. Pegenaute, and J. Rodriguez, El humo quirúrgico, riesgo laboral evaluable - revisión sistemática exploratoria de

- la bibliografía disponible, *Rev Asoc Esp Espec Med Trab* **31** (2022) 208, http://scielo.isciii.es/scielo.php?script=sci_arttext&pid=S3020-11602022000200008&Ing=es&nrm=iso.
5. Y. Tomita *et al.*, Mutagenicity of smoke condensates induced by CO₂-laser irradiation and electrocauterization, *Mutat Res* **89** (1981) 145, [https://doi.org/10.1016/0165-1218\(81\)90120-8](https://doi.org/10.1016/0165-1218(81)90120-8).
 6. D.S. Hill, J.K. O'Neill, R.J. Powell, and D.W. Oliver, Surgical smoke - A health hazard in the operating theatre: a study to quantify exposure and a survey of the use of smoke extractor systems in UK plastic surgery units, *J Plast Reconstr Aesthet Surg* **65** (2012) 911, <https://doi.org/10.1016/j.bjps.2012.02.012>.
 7. S. Gao, R.H. Koehler, M. Yermakov, and S.A. Grinshpun, Performance of facepiece respirators and surgical masks smoke: Simulated workplace protection factor study, *Ann Occup Hyg* **60** (2016) 608, <https://doi.org/10.1093/annhyg/mew006>.
 8. V.J. Casey, C. Martin, P. Curtin, K. Buckley, and L.M. McNamara, Comparison of surgical smoke generated during electrosurgery with aerosolized particulates from ultrasonic and high-speed cutting, *Ann Biomed Eng* **49** (2021) 560, <https://doi.org/10.1007/s10439-020-02587-w>.
 9. J.L. Fencl, Guideline implementation: Surgical smoke safety, *AORN J* **105** (2017) 488, <https://doi.org/10.1016/j.aorn.2017.03.006>.
 10. E.H. Benaim and I. Jaspers, Surgical smoke and its components, effects, and mitigation: a contemporary review, *Toxicol Sci* **198** (2024) 157, <https://doi.org/10.1093/toxsci/kfae005>.
 11. V.J. Casey and L.M. McNamara, Instrumental in Surgery: A narrative review on energy-based surgical cutting devices and surgical smoke, *Ann Surg* **278** (2023) e457, <https://doi.org/10.1097/SLA.0000000000005816>.
 12. F.J. Perez-Duarte *et al.*, Ergonomía en cirugía laparoscópica y su importancia en la formación quirúrgica, *Cir Esp* **90** (2012) 284, <https://doi.org/10.1016/j.ciresp.2011.04.021>.
 13. R. Berguer, W.D. Smith, and S. Davis, An ergonomic study of the optimum operating table height for laparoscopic surgery, *Surg Endosc* **16** (2002) 416, <https://doi.org/10.1007/s00464-001-8190-y>.
 14. N. Connor, ¿Qué es la aspereza relativa de la tubería? Definición, *Thermal Engineering*, 2020, <https://www.thermal-engineering.org/es/que-es-la-aspereza-relativa-de-la-tuberia-definicion/>.
 15. M.M. Binda, Humedification during laparoscopic surgery: overview of the clinical benefits of using humidified gas during laparoscopic surgery, *Arch Gynecol Obstet* **292** (2015) 955, <https://doi.org/10.1007/s00404-015-3717-y>.
 16. N. Mowbray, J. Ansell, N. Warren, P. Wall, and J. Torkington, Is surgical smoke harmful to theater staff? a systematic review, *Surg Endosc* **27** (2013) 3100, <https://doi.org/10.1007/s00464-013-2940-5>.
 17. I. Bröske-Hohlfeld *et al.*, Surgical smoke and ultrafine particles, *J Occup Med Toxicol* **3** (2008) 31, <https://doi.org/10.1186/1745-6673-3-31>.
 18. Y.Z. Zhou *et al.*, Surgical smoke: a hidden killer in the operating room, *Asian J Surg* **46** (2023) 3447, <https://doi.org/10.1016/j.asjsur.2023.03.066>.
 19. H. Carbajo-Rodríguez, J.L. Aguayo-Albasini, V. Soria-Aledo, and C. García-López, El humo quirúrgico: riesgos y medidas preventivas, *Cir Esp* **85** (2009) 274, <https://doi.org/10.1016/j.ciresp.2008.10.004>.
 20. Informe de prueba interno #RE00139506 rev. A, Bourbon: Informe de declaraciones realizadas por personal de enfermería y cirujanos sobre el sistema de extracción de humo laparoscópico Valleylab™, (2018).
 21. A.C. Kam, M. O'Brien, and P.C. Kam, Pleural drainage systems, *Anaesthesia* **48** (1993) 154, <https://doi.org/10.1111/j.1365-2044.1993.tb06859.x>.
 22. G. Birath and E.W. Swenson, Resistance to air flow in bronchospirometric catheters, *J Thorac Surg* **33** (1957) 275, [https://doi.org/10.1016/S0096-5588\(20\)30546-8](https://doi.org/10.1016/S0096-5588(20)30546-8).
 23. C.F. Colebrook and C.M. White, Experiments with fluid friction in roughened pipes. Proceedings of the Royal Society of London. Series A, *Mathematical and Physical Sciences* **161** (1937) 367, <https://doi.org/10.1098/rspa.1937.0150>.
 24. J. Vega, R. Valenzuela, and E. Ramírez, Manejo de las pleurostomías, *Rev Med Clin Condes* **29** (2018) 365, <https://doi.org/10.1016/j.rmclc.2017.07.013>.
 25. P. Xu, Y. Li, and J. Ren, Meta-analysis and systematic review of influence of different humidified carbon dioxide on intraoperative and postoperative gynaecological laparoscopic surgery, *Ann Palliat Med* **10** (2021) 7992, <https://doi.org/10.21037/apm-21-1517>.